

Science and Application of Oxyorthosilicate Nanophosphors

Ross E. Muenchausen, Edward A. McKigney, Luiz G. Jacobsohn, Michael W. Blair, Bryan L. Bennett, and D. Wayne Cooke

Abstract—Nanophosphor $\text{Y}_2\text{SiO}_5\text{:Ce}$ (*n*-YSO), $\text{Lu}_2\text{SiO}_5\text{:Ce}$ (*n*-LSO), and $\text{Gd}_2\text{SiO}_5\text{:Ce}$ (*n*-GSO) were prepared by solution-combustion synthesis yielding nanophosphor crystallite sizes between 20 nm – 80 nm. Ce dopant concentrations were varied between 0.1%–10% for each the nanophosphors and concentration quenching curves were measured by radioluminescence (RL) and photoluminescence (PL). *n*-YSO exhibits concentration quenching at 1 at% and 4 at% under uv and x-ray excitation, respectively. Red shifted emission with a larger Stokes shift is observed for nanophosphors as compared to bulk crystals. The measured PL lifetime depended on the refractive index of the media, indicating that the PL originates from the surface. Measurements of the RL/PL intensity indicate that the light output of these materials is comparable to the bulk crystal.

Index Terms—Concentration quenching, fluorescence lifetime, luminescence, nanophosphor, oxyorthosilicates.

I. INTRODUCTION

NANOMATERIALS are important because they exhibit novel electrical, optical and magnetic properties that are absent in their bulk counterparts and, therefore, offer new opportunities for device and application development. As physical size is reduced to the nanoscale regime (10^{-9} – 10^{-7} m), quantum effects, surface properties and interfacial interactions become dominant and the fundamental mechanisms that usually describe the “infinite solid” must be modified. The new “quantum-confined” behavior has led to a plethora of new nanoscale functional materials—porous silicon, carbon nanotubes, quantum dots/wires/wells—that offer myriad opportunities for technological advances, which will affect almost every aspect of life in the twenty-first century [1], [2].

Broad-based nanoscience research in photonics, magnetics, sensors, synthesis, and instrumentation is currently being aggressively pursued and exciting new results are rapidly emerging [3]. A particularly fruitful nanoscience research field is nanophotonics, an area that deals with fundamental processes of radiation-matter interaction on a scale that is much smaller than the wavelength of radiation [4]. Current nanophotonics research is primarily focused on exploitation of quantum confinement (QC) effects in semiconductors with attendant applications. Our work fits within a relatively new

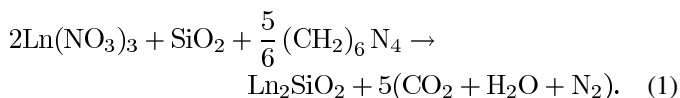
subfield—“nanophosphors”—which focuses on rare-earth doped *insulators* rather than *semiconductors*.

Rare-earth ions are excellent dopant probes as their energy levels typically reside within the band gap of insulators, and the highly localized *f* electrons are confined to dimensions much less than 1 nm, thus excluding QC effects. However, reduced dimensionality at nanometer scale is expected to confine phonons, which in turn may affect radiative vs. nonradiative relaxation rates [5].

In this paper, we summarize some initial findings regarding the optical behavior of a particular class of nanophosphors, the cerium-doped oxyorthosilicates $\text{Ln}_2\text{SiO}_5\text{:Ce}$ ($\text{Ln} = \text{Y, Gd, Lu}$) and compare their properties to single crystals. These materials are of particular interest for the detection of ionizing radiation as they are fast, bright and dense scintillators [6].

II. EXPERIMENTAL

Solution combustion synthesis (SCS) of both simple and complex oxide nanoparticles is well known [7], [8]. However, there are relatively few reports of SCS of silicates [9], and particularly oxyorthosilicates [10]. Nanophosphor powders were produced by the hexamine-nitrate solution combustion technique [11]. The stoichiometric combustion reaction is given by:



Three grams of Ln_2O_3 (> 99.9%) were dissolved in an excess of nitric acid (Baker, Huey HNO_3 , 65 wt%). Upon dissolution to a clear liquid, $\text{Ce}(\text{NO}_3)_3 \cdot 6\text{H}_2\text{O}$ was added; the dopant range was 0.1–10% for these studies. Stoichiometric fumed silica (Cab-O-Sil, 99.8% purity) was then mixed with the solution and hexamine $(\text{CH}_2)_6\text{N}_4$ (Baker, reagent grade) was added and the resultant mixture dried in a vacuum oven for 16 hrs. at 115°C . After drying, the powder was compacted into an unglazed alumina crucible and combusted in a muffle furnace preheated at 650°C . It was found that a 25% excess of fuel optimized the combustion, presumably to provide a longer burn for the solid-state reaction with the amorphous silica nanoparticles. The resulting ceramic foam was ground with a mortar and pestle and post-annealed at to 1000°C for 1 hr. to remove fuel and nitrate residues. However, it should be pointed out that the material was luminescent, though inhomogeneous, directly after the combustion process, and that x-ray diffraction (XRD) analysis showed no evidence of crystal growth due to annealing. For subsequent analysis, the nanopowders were uniaxially cold-pressed into 1 cm dia. by 2 mm pellets.

Manuscript received June 29, 2007; revised December 20, 2007. This research was supported in part by Laboratory Directed Research and Development funds and the DOE Office of Basic Energy Sciences.

The authors are with the Los Alamos National Laboratory, Los Alamos, NM 87544 USA (e-mail: rossm@lanl.gov).

Digital Object Identifier 10.1109/TNS.2008.922844

The structural characteristics of the nanopowders were investigated by θ -2 θ powder XRD and transmission electron microscopy (TEM). These measurements yielded the average crystallite size, size distribution, and crystallographic phase. TEM sample preparation consisted of evaporating a dilute suspension of nanoparticles directly onto a carbon-coated TEM grid. Photoluminescence excitation (PLE) and emission (PL) measurements were obtained in ambient conditions using a Photon Technology International TimeMasterTM fluorimeter. Radioluminescence (RL) spectral measurements were carried out under ambient conditions and have been described in detail elsewhere[twelve]

III. RESULTS AND DISCUSSION

XRD analysis of oxyorthosilicates produced by SCS indicated that these materials crystallize with monoclinic $P2_1/c$ structure, that corresponds to 7 and 9 oxygen coordinated Ln [13]. This is the same structure observed for bulk $Gd_2SiO_5:Ce$ (GSO) [14], but different than the $C2/c$ (6 and 7 oxygen coordinated) observed in bulk $Y_2SiO_5:Ce$ (YSO) and $Lu_2SiO_5:Ce$ (LSO). While this is consistent with the lower processing temperature of the SCS process ($< 1500^\circ\text{C}$) as compared to CZ crystal growth ($> 2000^\circ\text{C}$), additional process parameters such as the combustion temporal profile and O_2 concentration profile probably also play a role since nanocrystalline thin films of LSO:Ce, grown under equilibrium conditions of low temperature and low oxygen partial pressure exhibited $C2/c$ crystal structure [15]. The Debye-Scherrer analysis [16] yielded an average crystallite size of *ca.* 30 nm.

Nanophosphor oxyorthosilicate microstructure was further revealed through TEM. Fig. 1 is a TEM micrograph showing a typical grain of GSO. While the average crystallite size is consistent with the Debye-Scherrer analysis, TEM analysis revealed a broad size distribution, with dimensions typically ranging from 20 to 80 nm. The crystallites show no evidence of an amorphous core, indicating complete reaction. On the other hand, they have many dislocations and stacking faults, which is not unexpected for combustion produced materials [17]. A recent work using electron energy loss spectroscopy (EELS) in conjunction with STEM on $Y_2O_3:Tb$ nanophosphor confirms that the dopant is homogeneously distributed within the nanophosphor [18].

PL and PLE spectra of bulk and nanostructured (*n*-) YSO have been previously reported [13]. The nanophosphor PL spectrum exhibited a well-defined maximum at 431 nm ($\lambda_{\text{ex}} = 366$ nm) and is red shifted relative to the bulk spectrum. The broad spectrum of the bulk sample consists of peaks at 395 and 420 nm ($\lambda_{\text{ex}} = 356$ nm), which are attributed to the well-known emission from the spin-orbit split ground state of the $Ce^{3+}4f$ electron manifold [19]. The bulk PLE spectrum of bulk YSO is characterized by Ce^{3+} excitation bands at 356, 310 and 265 nm, which are associated with the crystal-field split $Ce^{3+}5d$ electronic levels. The *n*-YSO spectrum exhibited only the main excitation peak (366 nm) of the Ce^{3+} ion that was red shifted relative to the bulk peak.

An important question relates to the origin of the PL and PLE peak shifts being due to reduced dimensionality or simply due to

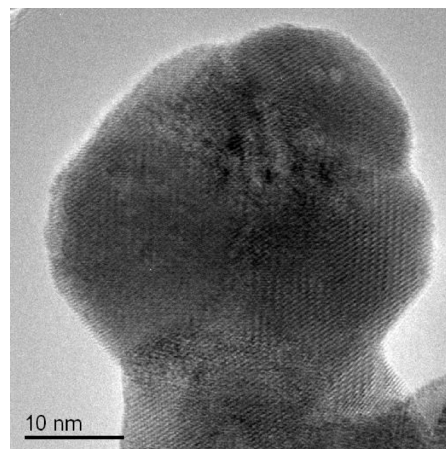


Fig. 1. High resolution transmission electron micrograph of a GSO crystallite produced by solution combustion synthesis.

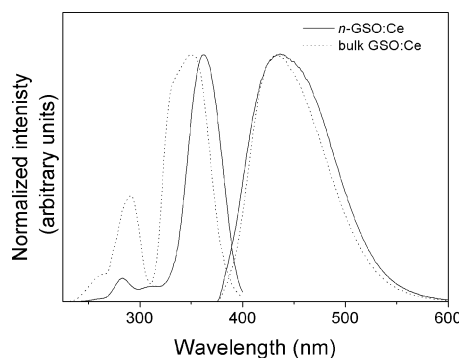


Fig. 2. PLE and PL spectra of bulk and *n*-GSO.

the change in crystal symmetry between the bulk and nanophosphor. Fortunately, bulk and *n*-GSO have the same structure. PLE/PL results for both are presented in Fig. 2. Note that PL and PLE data have been normalized for presentation purposes and thus absolute intensities cannot be compared. Similarly to *n*-YSO, red shifts are also observed in the PLE/PL in *n*-GSO. However, a much smaller red shift is observed in the PL of the *n*-GSO, 5 nm as compared to 20 nm for *n*-YSO [13]. The *n*-GSO PL red shift corresponds to a broadening of the emission peak to the red, which may be indicative of a greater contribution of emission from perturbed Ce sites in the nanophosphor as compared to the single crystal. This assertion is further supported by EPR of *n*-YSO:Ce and *n*-LSO:Ce, which show broader $Ce^{3+}(I)$ resonances, indicative of greater disorder in the nanophosphor. [20] We conclude that the PL and PLE of *n*-YSO with particle sizes 20–80 nm are primarily determined by the activator ion symmetry, though with smaller contribution due to reduced dimensionality.

Reduced dimensionality effects are more clearly manifested in the optical lifetime measurements of *n*-YSO. Ambient optical excitation at the main PLE bands of bulk and *n*-YSO powder yields fitted $1/e$ values of 39 and 55 ns, respectively. A method for measuring lifetime of powder specimens is to suspend the particles in a chemically inert solvent and magnetically stir them during optical excitation. In conducting these experiments we found that the nanophosphor lifetime was dependent upon the

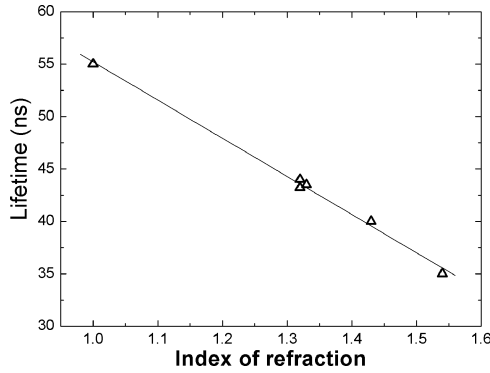


Fig. 3. Optical lifetime of *n*-YSO as a function of the embedding media.

medium in which it was immersed whereas the bulk YSO was independent of the medium. Similar effects observed in semi-conducting QD's and nanowires have been attributed to dielectric confinement, which is inversely related to the crystallite size [21]. Nanophosphor YSO lifetimes were measured in air (index of refraction $n = 1$), ethanol ($n = 1.32$), methanol ($n = 1.32$), de-ionized water ($n = 1.33$), dimethylformamide ($n = 1.43$) and epoxy ($n = 1.54$), and yielded fitted lifetimes 55.0, 44.0, 43.2, 43.5, 40.0 and 35.0 ns, respectively. All solvents showed negligible PL in the uv-vis region and an overall decrease in PL emission intensity with refractive index was observed for these samples. Typical error bar on these measurements is $\pm 3\%$. The results are plotted in Fig. 3.

Ce^{3+} emission is dominated by parity-allowed electric dipole transitions, with negligible nonradiative de-excitation by multiphonon relaxation. For a one-electron system the inverse radiative lifetime for transitions between initial and final states is given by [22]:

$$\frac{1}{\tau_{ij}} = \frac{n(n^2 + 2)^2}{9} \frac{e^2 f_{ij}}{2\pi\epsilon_0 mc\lambda^2} \quad (2)$$

with emission wavelength λ and oscillator strength f_{ij} . The first fraction in (2) is a correction to the local electric field seen by the Ce ion, which differs from the macroscopic electric field. The dielectric penetration has been estimated for nanoscale insulators and is reported to be between 30 nm [23], up to the emission wavelength [24]. For micron-size YSO the dielectric interaction between Ce ions and medium is negligible and n is simply the refractive index of the host lattice, *viz.* 1.82. In contrast, *n*-YSO:Ce will have a significant fraction of the Ce ions that can experience a local electric field induced by the surrounding medium. Therefore, the index of refraction to be used in (2) is not the value of YSO but to a first approximation taken as the value of the surrounding medium. Moreover, because λ is constant, we can extract f_{ij} from the experimentally determined lifetimes; the value is 0.013, which is in good agreement with reported values for Ce oscillator strengths [25]. A more accurate analysis, accounting for the host dielectric medium [24] has been performed which yielded a higher value of the oscillator strength [26].

It is well known that the optimum doping level in a phosphor depends on the rare-earth and host type. For nanophosphors, changes in the PL concentration quenching behavior has

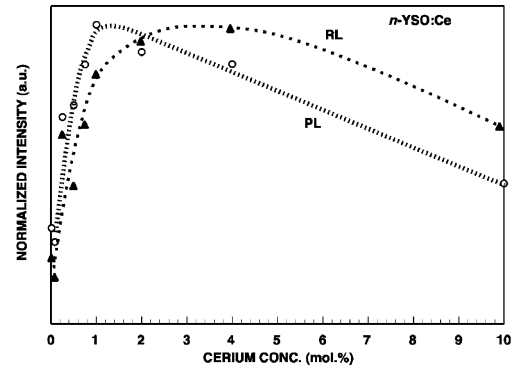


Fig. 4. Quenching curve for *n*-YSO:Ce measured under photoluminescence and radioluminescence excitation.

been reported for YSO:Eu [27], Y_2O_3 :Eu [28] and Y_2O_3 :Tb [29], where the general trend is that the peak in the nanophosphor quenching curve is shifted to higher concentrations with respect to the bulk materials. Less apparent is the observation that such behavior depends on the method of excitation, as shown in Fig. 4. The spectral band emission of the PL and RL were identical, although the exact peak position (red shifts) were systematically greater for the RL spectra. The PL peak concentration occurs around 1%, whereas the peak concentration inferred from RL excitation is significantly greater at 4%. In CZ grown oxyorthosilicates, the maximum Ce concentration is limited by the low segregation coefficient [30] to about 0.05%. Additional excitation dependent behavior is also associated with the measured light output of *n*-YSO as previously reported [13]. Under uv excitation the bulk and *n*-YSO:Ce intensities are the same. However, the mass normalized nanophosphor integrated light output is about three times greater than bulk powder, when excited by x-rays. As discussed previously [13], caution must be exercised when interpreting this result because 1) the nano and bulk material exhibit different crystal structures, 2) the Ce concentration is different for the nano and bulk material, 3) a larger Stokes shift in the nanophosphor, will reduce the self absorption and 4) variations in optical scattering due to different particle size, when measured by a fixed solid-angle detector, will effect the nano and bulk powder differently.

For scintillator applications, many more requirements must be met to successfully utilize nanophosphor powder. A nanocomposite will generally be required, especially for noncubic materials, such as LaCl_3 :Ce and LaBr_3 :Ce. The crystallites must be less than 20 nm [31] and well dispersed, the matrix material must not quench the inorganic nanophosphor and conversely, the nanophosphor must not quench the matrix material, if it is a scintillator. In subsequent work, we will report on our preliminary efforts to fabricate and characterize nanocomposite scintillators that fulfill these requirements.

IV. CONCLUSIONS

Based on the results briefly presented in this paper, we can conclude that nanophosphor optical properties are mostly determined by the local symmetry of the dopant ion, and that they depend on the method of excitation (PL, RL). PL and PLE

present red shift and greater Stokes shift in relation to bulk materials. The nanophosphor lifetime dependence on solvent refractive index implies that the PL emission is effected by the local electric field which penetrates throughout the nanoparticle. The observation that nanophosphor brightness is nominally equivalent to bulk materials is of great importance to technological applications.

ACKNOWLEDGMENT

The authors would like to acknowledge R. Wang and P.A. Crozier from Center for Solid State Science and School of Materials, Arizona State University, for EELS and HRTEM results.

REFERENCES

- [1] C. N. R. Rao and A. K. Cheetham, "Science and technology of nanomaterials: Current status and future prospects," *J. Mater. Chem.*, vol. 11, pp. 2887–2894, 2001.
- [2] P. Moriarty, "Nanostructured materials," *Rep. Prog. Phys.*, vol. 64, pp. 297–381, 2001.
- [3] H. Doumanidis, "The nanomanufacturing program at the National Science Foundation," *Nanotechnol.*, vol. 13, pp. 248–252, 2002.
- [4] Y. Shen, C. S. Friend, Y. Jiang, D. Jakubczyk, J. Swiatkiewicz, and P. N. Prasad, "Nanophotonics: Interactions, materials and applications," *J. Phys. Chem. B*, vol. 104, pp. 7577–7587, 2000.
- [5] B. Mercier, C. Dujardin, G. Ledoux, C. Louis, O. Tillement, and P. Perriat, "Confinement effects on sesquioxides," *J. Lumin.*, vol. 119–120, pp. 224–227, 2006.
- [6] E. Bescher, S. R. Robson, J. D. MacKenzie, B. Patt, J. Iwanczyk, and E. J. Hoffman, "New lutetium silicate scintillators," *J. Sol-Gel Sci. Technol.*, vol. 19, pp. 325–328, 2000.
- [7] S. Ekambaram, K. C. Patil, and M. Maaza, "Synthesis of lamp phosphors: Facile combustion approach," *J. Alloy Comp.*, vol. 393, pp. 81–92, 2005.
- [8] T. Mimani and K. C. Patil, "Solution combustion synthesis of nanoscale oxides and their composites," *Mater. Phys. Mech.*, vol. 4, pp. 134–137, 2001.
- [9] G. T. Chandrappa, S. Ghosh, and K. C. Patil, "Synthesis and properties of willemite," *J. Mater. Synth. Process.*, vol. 7, pp. 273–279, 1999.
- [10] E. J. Bosze, J. McKittrick, and G. A. Hirata, "Investigation of the physical properties of a blue-emitting phosphor produced using a rapid exothermic reaction," *Mater. Sci. Eng.*, vol. 97, pp. 265–274, 2003.
- [11] A. S. Prakash, A. M. A. Khadar, K. C. Patil, and M. S. Hegde, "Hexamethylenetetramine: A new fuel for solution combustion synthesis of complex metal oxides," *J. Mater. Synth. Process.*, vol. 10, pp. 135–141, 2002.
- [12] D. W. Cooke, B. L. Bennett, R. E. Muenchausen, J. K. Lee, and M. Nastasi, "Intrinsic ultraviolet luminescence from Lu_2O_3 , Lu_2SiO_5 and $\text{Lu}_2\text{SiO}_5 : \text{Ce}^{3+}$," *J. Lumin.*, vol. 106, pp. 125–132, 2004.
- [13] D. W. Cooke, J. K. Lee, B. L. Bennett, J. R. Groves, L. G. Jacobsohn, E. A. McKigney, R. E. Muenchausen, M. Nastasi, K. E. Sickafus, M. Tang, and J. A. Valdez, "Luminescent properties and reduced dimensional behavior of hydrothermally prepared Y_2SiO_5 : Ce nanophosphors," *Appl. Phys. Lett.*, vol. 88, pp. 103108–1–3, 2006.
- [14] H. Suzuki, T. A. Tombrello, C. L. Melcher, and J. S. Schweitzer, "UV and gamma-ray excited luminescence of cerium-doped rare-earth oxyorthosilicates," *Nucl. Instrum. Methods Phys. Res. A*, vol. 320, pp. 263–272, 1992.
- [15] J. K. Lee, R. E. Muenchausen, J. S. Lee, Q. X. Jia, M. Nastasi, J. A. Valdez, B. L. Bennett, D. W. Cooke, and S. Y. Lee, "Structure and optical properties of Lu_2SiO_5 :Ce phosphor thin films," *Appl. Phys. Lett.*, vol. 89, pp. 101905–1–3, 2006.
- [16] L. Alexander and H. P. Klug, "Determination of crystallite size with the x-ray spectrometer," *J. Appl. Phys.*, vol. 21, pp. 137–142, 1950.
- [17] C. Granquist, L. Kisyh, and W. Marlow, *Gas Phase Nanoparticle Synthesis*. Dordrecht, The Netherlands: Kluwer, 2004, ch. 3, sec. 4.4.
- [18] L. G. Jacobsohn, B. L. Bennett, R. E. Muenchausen, J. F. Smith, and D. W. Cooke, "Electron energy-loss spectroscopy investigation of dopant homogeneity in Tb-doped Y_2O_3 nanophosphor prepared by solution combustion," *J. Solid State Chem.*, submitted for publication.
- [19] G. Blasse and B. C. Grabmaier, *Luminescent Materials*. Berlin, Germany: Springer-Verlag, 1994, pp. 27–29.
- [20] D. W. Cooke, M. W. Blair, J. F. Smith, B. L. Bennett, L. G. Jacobsohn, E. A. McKigney, and R. E. Muenchausen, "EPR and luminescence of F^+ centers in bulk and nanophosphor oxyorthosilicates," presented at the IEEE SCINT, Winston-Salem, NC, 2007.
- [21] G. Goldoni, F. Rossi, and E. Molinari, "Strong exciton binding in quantum structures through remote dielectric confinement," *Phys. Rev. B*, vol. 80, pp. 4995–4998, 1998.
- [22] M. J. Weber, "Inorganic scintillators: Today and tomorrow," *J. Lumin.*, vol. 100, pp. 35–45, 2002.
- [23] R. Ramprasad and N. Shi, "Dielectric properties of nanoscale HfO_2 slabs," *Phys. Rev. B*, vol. 72, pp. 052107–1–4, 2005.
- [24] R. S. Meltzer, S. P. Feofilov, B. Tissue, and H. B. Yuan, "Dependence of fluorescence lifetimes of $\text{Y}_2\text{O}_3 : \text{Eu}^+$ nanoparticles on the surrounding medium," *Phys. Rev. B*, vol. 60, pp. R14012–15, 1999.
- [25] A. Lempicki and A. J. Wojtowicz, "Fundamental limitations of scintillators," *J. Lumin.*, vol. 60, pp. 942–947, 1994.
- [26] R. E. Muenchausen, L. G. Jacobsohn, B. L. Bennett, E. A. McKigney, J. F. Smith, and D. W. Cooke, "A novel method of extracting oscillator strength of select rare-earth ion optical transitions in nanostructured dielectric materials," *Solid State Commun.*, vol. 139, pp. 497–500, 2006.
- [27] W. Zhang, P. Xie, C. Duan, K. Yan, M. Yin, L. Lou, S. Xia, and J.-C. Krupa, "Preparation and size effects on concentration quenching of nanocrystalline Y_2SiO_5 :Eu," *Chem. Phys. Lett.*, vol. 292, pp. 133–136, 1998.
- [28] W.-W. Zhang, W.-P. Zhang, P.-B. Xie, M. Yin, H.-T. Chen, L. Jing, Y.-S. Zhang, L.-R. Lou, and S.-D. Xia, "Optical properties of nanocrystalline Y_2O_3 :Eu depending on its odd structure," *J. Coll. Inter. Sci.*, vol. 262, pp. 588–593, 2003.
- [29] R. E. Muenchausen, L. G. Jacobsohn, B. L. Bennett, E. A. McKigney, J. F. Smith, J. A. Valdez, and D. W. Cooke, "Effects of Tb doping on the photoluminescence of Y_2O_3 :Tb nanophosphors," *J. Lumin.*, vol. 127, pp. 838–842, 2007.
- [30] D. W. Cooke, K. J. McClellan, B. L. Bennett, J. M. Roper, M. T. Whittaker, R. E. Muenchausen, and R. C. Sze, "Crystal growth and optical characterization of cerium-doped $\text{Lu}_{1.8}\text{Y}_{0.2}\text{SiO}_5$," *J. Appl. Phys.*, vol. 88, pp. 7360–7362, 2000.
- [31] E. A. McKigney, R. E. Del Sesto, L. G. Jacobsohn, P. A. Santi, R. E. Muenchausen, K. C. Ott, T. M. McCleskey, B. L. Bennett, J. F. Smith, and D. W. Cooke, "Nanocomposite scintillators for radiation detection and nuclear spectroscopy," *Nucl. Instrum. Meth. Phys. Res. A*, to be published.